AD-A141 950 IMPROVED LONG-WAVELENGTH DISPERSION RELATION FOR THE NEGATIVE MASS INSTAB..(U) MISSION RESEARCH CORP ALBUQUERQUE NM B B GODFREY ET AL. NOV 83 AMRC-R-520 1/1

UNCLASSIFIED N00014-84-C-0078 F/G 20/7 NL

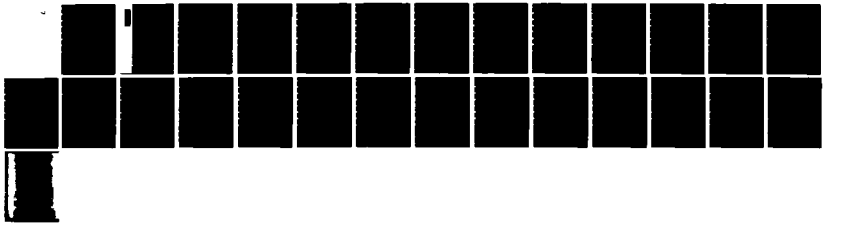

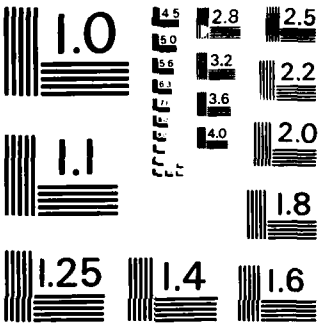

AMRC-R-520
Copy 12

IMPROVED LONG-WAVELENGTH DISPERSION RELATION FOR THE NEGATIVE MASS INSTABILITY IN HIGH CURRENT CONVENTIONAL AND MODIFIED BETATRONS

B. B. Godfrey
T. P. Hughes

November 1983

Prepared for: Office of Naval Research
Physical Sciences Division
800 North Quincy Street
Arlington, Virginia 22217

Under Contract: N00014-84-C-0078

Prepared by: MISSION RESEARCH CORPORATION
1720 Randolph Road, S.E.
Albuquerque, New Mexico 87106

UNCLASSIFIED

SECURITY CLASSIFICATION OF THIS PAGE (When Data Entered)

REPORT DOCUMENTATION PAGE	READ INSTRUCTIONS BEFORE COMPLETING FORM
1. REPORT NUMBER	2. GOVT ACCESSION NO. AD-A141950	3. RECIPIENT'S CATALOG NUMBER
4. TITLE (and Subtitle) IMPROVED LONG-WAVELENGTH DISPERSION RELATION FOR THE NEGATIVE MASS INSTABILITY IN HIGH CURRENT CONVENTIONAL AND MODIFIED BETATRONS	5. TYPE OF REPORT & PERIOD COVERED INTERIM 6. PERFORMING ORG. REPORT NUMBER AMRC-R-520
7. AUTHOR(s) B. B. Godfrey T. P. Hughes	8. CONTRACT OR GRANT NUMBER(s) N00014-84-C-0078
9. PERFORMING ORGANIZATION NAME AND ADDRESS MISSION RESEARCH CORPORATION 1720 Randolph Road, S.E. Albuquerque, New Mexico 87106	10. PROGRAM ELEMENT, PROJECT, TASK AREA & WORK UNIT NUMBERS
11. CONTROLLING OFFICE NAME AND ADDRESS Office of Naval Research 800 North Quincy Street Arlington, Virginia 22217	12. REPORT DATE November 1983 13. NUMBER OF PAGES 25
14. MONITORING AGENCY NAME & ADDRESS(if different from Controlling Office)	15. SECURITY CLASS. (of this report) Unclassified 15a. DECLASSIFICATION DOWNGRADING SCHEDULE

16. DISTRIBUTION STATEMENT (of this Report)

Approved for Public Release - Distribution Unlimited.

17. DISTRIBUTION STATEMENT (of the abstract entered in Block 20, if different from Report)

18. SUPPLEMENTARY NOTES

19. KEY WORDS (Continue on reverse side if necessary and identify by block number)

High Current Betatron
Racetrack Induction Accelerator
Negative Mass Instability

20. ABSTRACT (Continue on reverse side if necessary and identify by block number)

A new linear dispersion relation, taking proper account of toroidal curvature effects on the electromagnetic fields, has been derived for the negative mass instability in high current betatrons. (The low frequency and paraxial approximations are employed.) The dispersion relation typically gives growth rates which are smaller than those from earlier analyses and are in better agreement with simulation code results. Applying these findings to the Office of Naval Research racetrack induction accelerator design suggests that it may be safe from severe negative mass instability development with only a modest

DD FORM 1 JAN 73 1473 EDITION OF 1 NOV 65 IS OBSOLETE

UNCLASSIFIED

SECURITY CLASSIFICATION OF THIS PAGE (When Data Entered)

TABLE OF CONTENTS

A1

I. INTRODUCTION

An accurate cold beam linear dispersion relation for the negative mass instability in high current conventional or modified betatrons is critical for designing experiments, benchmarking computer simulations, and developing warm beam dispersion relations. In this report we derive a dispersion relation correct to first order in the toroidal aspect ratio of the betatron valid for small toroidal mode numbers. Limited comparisons with earlier work are provided for reference.

The two earlier treatments of negative mass instability growth in high current betatrons included toroidal curvature effects in the particle dynamics but not in the electromagnetic field equations.[1,2] In other words, the dispersion relations were derived for beam motion in a toroidal cavity but with fields computed for an off-center beam in a straight tube of circular crossection. The first analysis, that of Sprangle and Vomvoridis, used an equation of continuity appropriate to a straight cylinder, as well. In contrast, the second analysis, due to Hughes and Godfrey, incorporated an equation of continuity correct for a toroidal beam. Predicted growth rates from these two models often have been found to disagree by factors of two for parameters corresponding to peak growth and by even more at higher beam energies. More disturbingly, both models systematically overestimate instability growth rates observed in three-dimensional computer simulations.[3,4] We attribute these discrepancies to incomplete treatment of toroidal curvature effects.

The dominant curvature correction to the field equations is easily identified. Radial motion of an electron ring (see Fig. 1) gives rise to azimuthal bunching. This constitutes the difference between charge continuity in cylindrical and toroidal geometry. Conversely, azimuthal bunching gives rise to a radial electric field, which constitutes the (main) difference between electromagnetic fields in cylindrical and toroidal geometry.

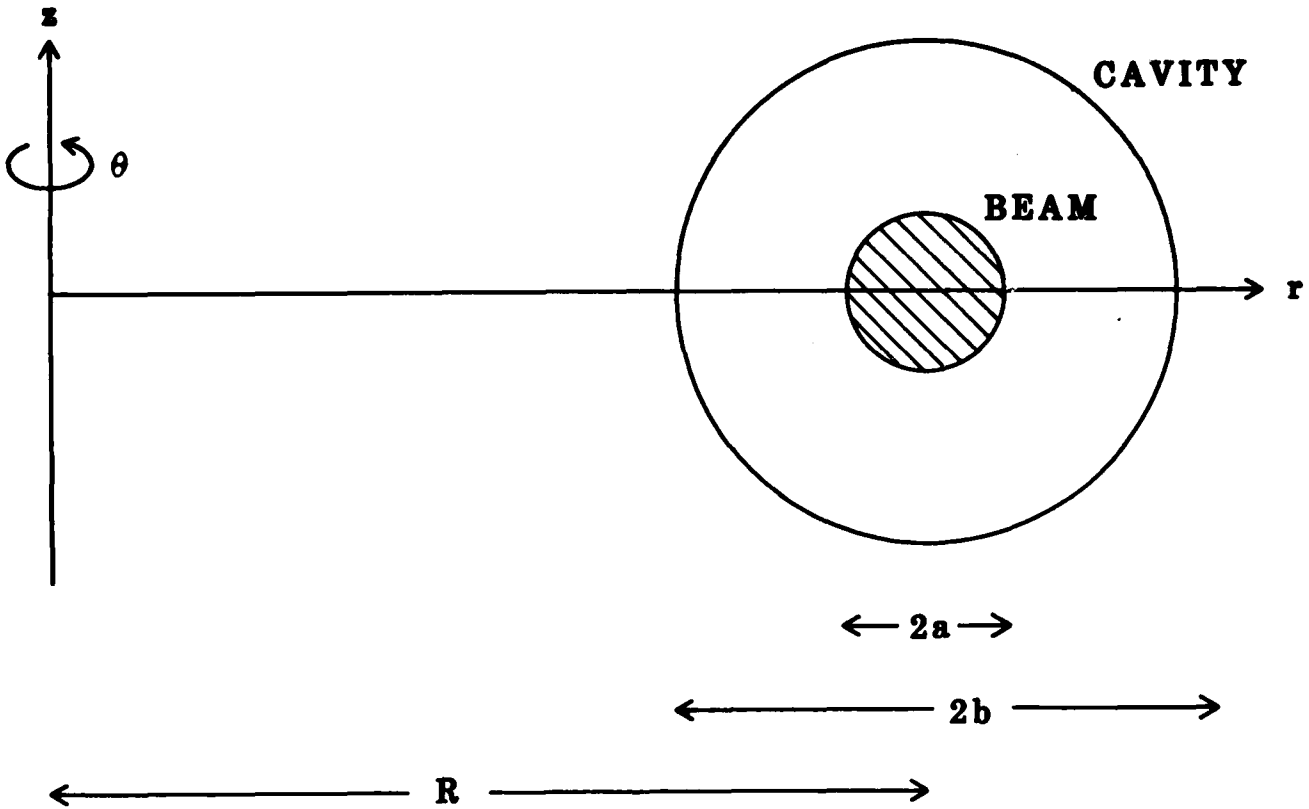

Figure 1. Schematic representation of betatron cavity with electron beam. Mirror and optional toroidal magnetic fields are applied.

The additional coupling between radial and azimuthal beam motion need not be small. Indeed, for sufficiently large energies this coupling through the fields must dominate coupling through the particle dynamics. The latter falls off with energy, while the former does not.

The present paper includes these and other (lesser) curvature effects to first order in the equilibrium and perturbed fields, producing what we believe to be a more accurate dispersion relation. Like its predecessors, this analysis ignores the internal dynamics of the beam, treating it as a string of rigid disks. The assumption of long azimuthal wavelengths also is implicit in our derivation. Relaxing the last constraint is conceptually straightforward but algebraically difficult.

In Section II we assemble the various particle and field equations into a 5×5 self-adjoint matrix operator acting on the perturbed beam centroid position and the electrostatic and electromagnetic potentials. The differential equations are solved to first order in the toroidal aspect ratio in Section III, and the remaining algebraic equations collapsed to the desired dispersion relation. When no toroidal magnetic field exists (i.e., for a conventional betatron), an analytic growth rate expression for the negative mass instability, valid over a wide parameter range, can be derived from the general dispersion relation, and this is done in Section IV. We have not yet attempted to obtain a corresponding simple growth rate expression for the modified betatron.

Finally, Section V presents a reevaluation of negative mass growth for the Office of Naval Research racetrack induction accelerator design,[5] based on the new dispersion relation. The average instability growth rate during acceleration from a few to 50 MeV is reduced by a factor of two relative to an earlier prediction.[6] With this improvement, the proposed accelerator may be able to "outrun" the instability with only a modest beam thermal energy spread.[7]

Comparisons with computer simulation results, as applied to the Naval Research Laboratory modified betatron design, are described elsewhere.[8]

II. FORMULATION OF THE PROBLEM

We consider an electron ring circulating in an azimuthally symmetric conducting cavity. Dimensions and coordinates are depicted in Figure 1. For the present we assume only that the beam and cavity crossections are symmetric about z=0. Otherwise, the crossections may assume any reasonable shape. The characteristic minor radius of the beam must be much less than that of the cavity so that the internal dynamics of the beam can be ignored. A mirror magnetic field maintains the beam in a circular orbit, and a toroidal field can be added to confine the beam against its self-fields, which need not be small.

Linearized equations for small transverse displacements of the beam centroid are easily obtained from the single particle equations of motion.

$$\gamma\, \delta\ddot{z} = \delta E_z - V_\theta\, \delta B_r + B_\theta\, \delta\dot{r} + \left(\frac{\partial E_z}{\partial z} - V_\theta \frac{\partial B_r}{\partial z} \right) \delta z \qquad (1)$$

$$\gamma\, \delta\ddot{r} = \delta E_r + V_\theta\, \delta B_z - B_\theta\, \delta\dot{z} + \left(\frac{\partial E_r}{\partial r} + V_\theta \frac{\partial B_z}{\partial r} - \frac{\gamma V_\theta^2}{R^2} \right) \delta r$$

$$+ \left(\left(\gamma^2 + 1 \right) \frac{\gamma V_\theta}{R^2} + B_z \right) \delta V_\theta \qquad (2)$$

Perturbed quantities are preceded by a delta (e.g., δz), while unperturbed quantities are not. Total time derivatives of perturbed particle quantities are represented by dots above the quantities (e.g. $\delta\ddot{z}$). Note that the last term in Eq. (2) can be rearranged, if desired, by means of the equilibrium radial force balance equation,

$$E_r + V_\theta B_z + \gamma V_\theta^2 / R = 0 \qquad (3)$$

Although the perturbed azimuthal velocity equation can be derived in many ways, using the single particle energy formula seems simplest.

$$\gamma^3 \delta\dot{V}_\theta = \delta E_\theta + \frac{E_r}{V_\theta} \delta r \tag{4}$$

The perturbed azimuthal angle $\delta\theta$ of a beam disk is related to δV_θ by

$$\delta V_\theta = R \, \delta\dot{\theta} + \frac{V_\theta}{R} \delta r \tag{5}$$

Perturbed beam currents resulting from the centroid displacements described by Eq. (1), (2), (4), and (5) are

$$\delta J_r = \rho \, \delta\dot{r}, \quad \delta J_z = \rho \, \delta\dot{z}$$

and

$$\delta J_\theta = \rho \, \delta V_\theta + V_\theta \, \delta\rho \tag{6}$$

Perturbed charge density is, in turn, derived by substituting the perturbed currents into the continuity equation and integrating the result in time.

$$\delta\rho + \frac{\partial}{\partial\theta} \rho\delta\theta + \frac{1}{r} \frac{\partial}{\partial r} r \, \rho\delta r + \frac{\partial}{\partial z} \rho\delta z = 0 \tag{7}$$

Alternatively, Eq. (7) can be obtained by considering how the density of a beam element changes as it is displaced infinitesimally in each direction.

As explained in the Introduction, we are limiting consideration to low frequencies and long azimuthal wavelengths. In this limit we need only determine the electrostatic and azimuthal electromagnetic potentials, which satisfy

$$\left(\frac{1}{r} \frac{\partial}{\partial r} r \frac{\partial}{\partial r} + \frac{\partial^2}{\partial z^2} \right) \delta\phi = - \delta\rho \tag{8}$$

$$\left(\frac{\partial}{\partial r} \frac{1}{r} \frac{\partial}{\partial r} r + \frac{\partial^2}{\partial z^2} \right) \delta A = - \delta J_\theta \tag{9}$$

The electric and magnetic field combinations appearing in Eq. (1), (2), and (4) are expressed in terms of these potentials as

$$\delta E_z - V_\theta \delta B_r = - \frac{\partial}{\partial z} \delta\phi + V_\theta \frac{\partial}{\partial z} \delta A \tag{10}$$

$$\delta E_r + V_\theta \delta B_z = - \frac{\partial}{\partial r} \delta\phi + V_\theta \frac{1}{r} \frac{\partial}{\partial r} r \delta A \tag{11}$$

$$\delta E_\theta = - \frac{1}{r} \frac{\partial}{\partial \theta} \delta\phi - \frac{\partial}{\partial t} \delta A \tag{12}$$

These equations complete our model.

Let us now cast the equations in matrix form for compactness and to emphasize their symmetry. In so doing we also Fourier transform the equations in time and azimuthal angle, i.e.,

$$\frac{\partial}{\partial t} \rightarrow -i\omega, \qquad \frac{\partial}{\partial \theta} \rightarrow i\ell$$

and eliminate δV_θ and the perturbed electric and magnetic fields.

$$
\begin{bmatrix}
\alpha_z & -i\Omega B_\theta & 0 & -\frac{\partial}{\partial z} & V_\theta \frac{\partial}{\partial z} \\
i\Omega B_\theta & \alpha_r & -i\Omega\beta & -\frac{\partial}{\partial r} & V_\theta \frac{1}{r} \frac{\partial}{\partial r} r \\
0 & i\Omega\beta & \Omega^2\gamma^3 & -i\frac{\ell}{r} & i\omega \\
\frac{\partial}{\partial z}\rho & \frac{1}{r}\frac{\partial}{\partial r} r\rho & \frac{i\ell}{r}\rho & -\left(\frac{1}{r}\frac{\partial}{\partial r} r \frac{\partial}{\partial r} + \frac{\partial^2}{\partial z^2}\right) & 0 \\
-V_\theta \frac{\partial}{\partial z}\rho & -V_\theta \frac{\partial}{\partial r}\rho & -i\omega\rho & 0 & \left(\frac{\partial}{\partial r}\frac{1}{r}\frac{\partial}{\partial r} r + \frac{\partial^2}{\partial z^2}\right)
\end{bmatrix}
\begin{bmatrix}
\delta z \\ \delta r \\ r\delta\theta \\ \delta\phi \\ \delta A
\end{bmatrix}
$$

$$
= 0 \qquad (13)
$$

Note that the matrix operator is self-adjoint, as one would hope. Certain symbols appearing in Eq. (13) are defined as

$$
\alpha_z \equiv \gamma\Omega^2 + \frac{\partial E_z}{\partial z} - V_\theta \frac{\partial B_r}{\partial z} \qquad (14)
$$

$$
\alpha_r \equiv \gamma\Omega^2 + \frac{\partial E_r}{\partial r} + V_\theta \frac{\partial B_z}{\partial r} + \frac{V_\theta}{R}\left(\gamma^3 \frac{V_\theta}{R} + B_z\right) \qquad (15)
$$

$$
\beta \equiv \gamma^3 \frac{V_\theta}{R} - \frac{E_r}{V_\theta} \qquad (16)
$$

$$
\Omega \equiv \omega - \ell \frac{V_\theta}{R} \qquad (17)
$$

Equation (13) can be solved numerically for beams and cavities of arbitrary cross section. (Before doing so, it probably would be desirable to perform a conformal transformation on r,z to map the beam and cavity boundaries onto coordinate surfaces.) In the next Section we instead assume the beam and cavity to be circular and concentric in cross section, as illustrated in Fig. 1, in order to obtain an analytical dispersion relation. We should bear in mind, however, that other configurations may exhibit improved stability.

III. DERIVATION OF THE DISPERSION RELATION

To develop a dispersion relation from Eq. (13), even for the simple geometry explicitly represented by Fig. 1, is a long and involved process. For the sake of brevity, we here restrict ourselves to outlining the procedure and citing pertinent results.

Converting the partial differential operators in Eq. (13) to a set of coupled ordinary differential operators is the first step. To do this we carry out the coordinate transformation

$$z = x\cos\psi, \quad r = R + x\sin\psi$$

and expand the potentials as Fourier series in poloidal angle ψ.

$$\delta\phi = \sum\delta\phi^m(x)\, e^{im\psi}, \qquad \delta A = \sum\delta A^m(x)\, e^{im\psi}$$

Next, we recast Eq. (13) as a variational integral, insert the $\delta\phi$ and δA expansions, explicitly integrate over ψ, and perform variations with respect to $\delta\phi^m$ and δA^m. This results in an infinite set of differential equations in $\underline{x}$ coupling all the poloidal modes of the potentials.

Expanding the differential equations in x with respect to the cavity aspect ratio, b/R, leads to a natural truncation of the infinite system. Basically, an expansion to order $|m|$ in b/R is consistent with dropping all higher poloidal mode numbers. Two orderings spring to mind. In the first ω, ℓ/R and the electron oscillation frequencies all are taken to be of order unity (or smaller), and the equations expanded to order b/R. In the second, ω and ℓ/R are taken to be of order b/R, and the equations expanded to b^2/R^2. The first alternative is much simpler, seems to capture the essential physics, and agrees reasonably well with simulation results, so we use it in the following calculations. We are, however, investigating the consequences of the second ordering and will publish our findings at a later date.

With the ordering selected, straightforward but tedious calculations yield for $x < a$:

$$\delta\phi \approx \frac{1}{4}\left(i\frac{\ell}{R}\rho R\delta\theta + \frac{1}{R}\rho\delta r\right)\left(x^2 - a^2\left(1 + 2\ell n\frac{b}{a}\right)\right)$$

$$+ \frac{1}{8R}\rho\delta r\left(-x^2\left(1 - \frac{a^2}{b^2}\right) + 2a^2\ell n\frac{b}{a}\right)$$

$$+ \frac{1}{2}\left(1 - \frac{a^2}{b^2}\right)\rho\delta r \times \sin\psi$$

$$+ \frac{1}{16R} i\frac{\ell}{R}\rho R\delta\theta\left(-x + a^2\left(\frac{a^2}{b^2} + 4\ell n\frac{b}{a}\right)\right) \times \sin\psi$$

$$+ \frac{1}{2}\left(1 - \frac{a^2}{b^2}\right)\rho\delta z \times \cos\psi \qquad (18)$$

$$\delta A \approx \frac{1}{4} i\omega\rho R\delta\theta\left(x^2 - a^2\left(1 + 2\ell n\frac{b}{a}\right)\right)$$

$$+ \frac{V_\theta}{8R}\rho\delta r\left(-x^2\left(1 - \frac{a^2}{b^2}\right) + 2a^2\ell n\frac{b}{a}\right)$$

$$+ \frac{V_\theta}{2}\left(1 - \frac{a^2}{b^2}\right)\rho\delta r \times \sin\psi$$

$$+ \frac{1}{16R} i\omega\rho R\delta\theta\left(x^2 + a^2\left(3\frac{a^2}{b^2} - 4 + 4\ell n\frac{b}{a}\right)\right) \times \sin\psi$$

$$+ \frac{V_\theta}{2}\left(1 - \frac{a^2}{b^2}\right)\rho\,\delta z \times \cos\psi \qquad (19)$$

The validity of these solutions to the truncated equations has been verified using the symbolic manipulation program MAXIMA.

Back substitution of the potentials into the variational integral allows the remaining integrations to be carried out explicitly. (For consistency, the results are truncated to first order in b/R.) Again, MAXIMA was used to check the manipulations. The resulting matrix equations for the perturbed centroid location appear as Eq. (20). Its determinant is the sought-for dispersion relation.

$$\begin{bmatrix} \alpha_z - \frac{\rho}{2\gamma^2}\left(1-\frac{a^2}{b^2}\right) & -i\Omega B_\theta^\circ & 0 \\ i\Omega B_\theta^\circ & \alpha_r - \frac{\rho}{2\gamma^2}\left(1-\frac{a^2}{b^2}\right) & -i\Omega\beta - i\frac{\rho a^2}{16R}\cdot\left[\omega V_\theta\left(3-3\frac{a^2}{b^2}+4\ell n\frac{b}{a}\right)+\frac{\ell}{R}\left(1+\frac{a^2}{b^2}+4\ell n\frac{b}{a}\right)\right] \\ 0 & i\Omega\beta + i\frac{\rho a^2}{16R}\cdot\left[\omega V_\theta\left(3-3\frac{a^2}{b^2}+4\ell n\frac{b}{a}\right)+\frac{\ell}{R}\left(1+\frac{a^2}{b^2}+4\ell n\frac{b}{a}\right)\right] & \Omega^2\gamma^3 + \frac{\rho a^2}{8}\left(\omega^2-\frac{\ell^2}{R^2}\right)\left(1+4\ell n\frac{b}{a}\right) \end{bmatrix} \begin{bmatrix} \delta z \\ \delta r \\ R\delta\theta \end{bmatrix}$$

$$= 0 \qquad (20)$$

In evaluating the matrix elements, it is necessary to know the equilibrium fields. They are[9]

$$E_r = \frac{\rho}{2}(r-R) + \frac{\rho a^2}{16R}\left(\frac{a^2}{b^2} + 4\,\ell n\,\frac{b}{a}\right) \tag{21}$$

$$B_z = -V_\theta\,\frac{\rho}{2}\,(r-R) + V_\theta\,\frac{\rho a^2}{16R}\left(-\frac{a^2}{b^2} + 4 + 4\,\ell n\,\frac{b}{a}\right)$$

$$+\; B_z^\circ\left(1 - n\,\frac{r-R}{R}\right) \tag{22}$$

with similar expressions for E_z and B_r. Eq. (3) determines the magnitude of B_z°, and B_θ° is arbitrary.

The dispersion relation is

$$\left(\Omega^2 - \omega_z^2\right)\left(\Omega^2 - \omega_r^2 - \chi/\varepsilon\right) - \Omega^2\,B_\theta^{\circ 2}/\gamma^2 = 0 \tag{23}$$

It represents two longitudinal ($m = 0$) modes, described by the longitudinal dielectric constant,

$$\varepsilon \equiv \Omega^2 - \frac{\nu}{\gamma^3}\left(\frac{1}{2} + 2\,\ell n\,\frac{b}{a}\right)\left(\frac{\ell^2}{R^2} - \omega^2\right) \tag{24}$$

and four transverse ($m = \pm 1$) modes, described by Eq. (23) with $\chi = 0$. The transverse oscillation frequencies ω_z and ω_r are,

$$\omega_z^2 \equiv -n\,V_\theta\,\frac{B_z^\circ}{\gamma R} - \frac{2\nu}{\gamma^3 b^2} \tag{25}$$

$$\omega_r^2 \equiv -(1-n)\ V_\theta \frac{B_z^\circ}{\gamma R} - \frac{2\nu}{\gamma^3 b^2} - \frac{B_z}{\gamma R} - \frac{2E_r}{\gamma R} + \left(\frac{E_r}{\gamma^2 V_\theta}\right)^2 \quad (26)$$

E_r and B_z in Eq. (26) are given by Eq. (21) and (22) with r=R and B_z° omitted. The last term in Eq. (26) is very small. Typically, the external field index n is chosen such that $\omega_r^2 \approx \omega_z^2$. Note that ν is Budker's parameter, equal to $\rho a^2/4$.

The key result of our analysis is the coupling coefficient between longitudinal and transverse modes, which determines the negative mass instability growth rate.

$$\chi \equiv \left\{\left(\frac{\gamma V_\theta}{R} - \frac{E_r}{\gamma^2}\right)\Omega + \frac{\nu}{\gamma^2}\frac{1}{4R}\left[\omega V_\theta\left(3 - 3\frac{a^2}{b^2} + 4\,\ell n\,\frac{b}{a}\right) + \frac{\ell}{R}\left(1 + \frac{a^2}{b^2} + 4\,\ell n\,\frac{b}{a}\right)\right]\right\}^2 - \left(\frac{\gamma V_\theta}{R} - \frac{E_r}{\gamma^2}\right)^2 \varepsilon \quad (27)$$

For comparison, the dispersion relations from Ref. 1 and 2 also can be cast in the form of Eq. (23) but with coupling coefficients, respectively,

$$\chi \equiv \left(\frac{\gamma V_\theta}{R}\right)^2 (\Omega^2 - \varepsilon) \quad (28)$$

and

$$\chi \equiv \frac{\gamma V_\theta}{R}\,\Omega\left[\frac{\gamma V_\theta}{R}\,\Omega + \frac{\ell}{R^2}\,\frac{\nu}{\gamma^2}\left(1 + 2\,\ell n\,\frac{b}{a}\right)\right] - \left(\frac{\gamma V_\theta}{R}\right)^2 \epsilon \qquad (29)$$

It should be noted that there is a degree of arbitrariness in the choice for the functional form of $\rho(r,z)$. In the preceding analysis we assumed ρ to be constant out to the beam minor radius a, where it drops abruptly to zero. One might instead have chosen $\rho r/R$ to be constant, for instance.[9] Fortunately, such changes lead only to insignificant modifications of χ, ω_z^2, and ω_r^2.

IV. $B_\theta^\circ = 0$ GROWTH RATE FORMULA

In the absence of a toroidal magnetic field, the negative mass instability dispersion relation reduces to

$$\Omega^2 - \omega_r^2 - \chi/\varepsilon = 0 \tag{30}$$

A simple analytical growth rate expression can be derived from Eq. (30) in a reasonably straightforward manner, if Ω^2 is much less than ω_r^2 and can be dropped from the equation. We address the validity of this assumption at the end of this Section.

Solely for the sake of algebraic simplicity, we invoke four approximations.

$$\frac{1}{\gamma^2} \ll 1$$

$$\frac{\nu}{\gamma^3}\left(1 + 2\ell n \frac{b}{a}\right) \ll 1$$

$$\frac{a^2}{b^2} \ll 1$$

$$\frac{E_r}{\gamma^2} \ll \gamma \frac{V_\theta}{R}$$

All four are well satisfied for typical cases of interest. Then,

$$\varepsilon \approx \Omega^2 + 2\Omega \frac{V_\theta}{R} \frac{\nu}{\gamma^3}\left(\frac{1}{2} + 2\ell n \frac{b}{a}\right) - \frac{\ell^2}{R^2} \frac{\nu}{\gamma^5}\left(\frac{1}{2} + 2\ell n \frac{b}{a}\right) \tag{31}$$

$$\chi \approx \left[\gamma \frac{V_\theta}{R}\Omega + \frac{\ell}{R^2}\frac{\nu}{\gamma^2}\left(1 + 2\ell n \frac{b}{a}\right)\right]^2$$

$$- \left(\gamma \frac{V_\theta}{R}\right)^2 \varepsilon \qquad (32)$$

Significant cancellations occur when Eq. (32) is expanded.

$$\chi \approx \Omega \frac{V_\theta}{R}\frac{\ell}{R^2}\frac{\nu}{\gamma} + \frac{V_\theta^2}{R^2}\frac{\ell^2}{R^2}\frac{\nu}{\gamma^3}\left(\frac{1}{2} + 2\ell n \frac{b}{a}\right) \qquad (33)$$

The term linear in Ω, in fact, only survives due to the difference in the factors

$$1 + 2\ell n \frac{b}{a}, \quad \frac{1}{2} + 2\ell n \frac{b}{a}$$

which appear in the first and second terms, respectively, of the definition for χ. Modifications to the expression for χ discussed near the end of the preceding Section, due to changing the functional form of ρ, are of higher order than the terms in Eq. (33) and so drop out. Nonetheless, we should not be surprised if more accurate dispersion relation derivations, perhaps including high frequency electromagnetic effects, adjust the linear term somewhat.

Substitution of Eq. (31) and (33) into

$$\omega_r^2 \varepsilon + \chi = 0$$

leads immediately to the desired growth rate formula.

$$\Omega \approx \frac{1}{1-n}\frac{\ell}{R}\left\{-\frac{\nu}{2\gamma} \pm i\left[\left(1-n\right)\frac{\nu}{\gamma^3}\left(\frac{1}{2} + 2\ell n \frac{b}{a}\right) - \left(\frac{\nu}{2\gamma}\right)^2\right]^{1/2}\right\} \qquad (34)$$

In obtaining Eq. (34), we have taken

$$\omega_r^2 \approx (1-n)\ \frac{V_\theta^2}{R^2}\ ,$$

which is accurate for γ^2 not too small, an assumption we have already made. Equation (34) reproduces the exact numerical solutions of the dispersion relation presented in the next Section to an accuracy of 10%.

Equation (34) predicts an instability cutoff for

$$\nu\gamma > 4(1 - n)\ \left(\frac{1}{2} + 2\ell n\ \frac{b}{a}\right) \tag{35}$$

At smaller values of $\nu\gamma$, the negative mass instability reduces to the well known expression[10,11]

$$\Gamma = \frac{\ell}{R}\left[\frac{1}{1-n}\ \frac{\nu}{\gamma^3}\ \left(\frac{1}{2} + 2\ell n\ \frac{b}{a}\right)\right]^{1/2} \tag{36}$$

We remark for completeness that Eq. (28), from Ref. 1, and Eq. (29), from Ref. 2, also yield high $\nu\gamma$ cutoffs. In the case of Eq. (29) instability ceases for[2,12]

$$\nu\gamma\ >\ 4(1 - n)/(1 + 2\ell n\ \frac{b}{a}) \tag{37}$$

while Eq. (28) has the same limit without the factor of four. Both analyses lead to Eq. (36) for sufficiently small $\nu\gamma$.

Let us return to our initial assumption,

$$\Omega^2 \ll \omega_r^2$$

Based on Eq. (34), this inequality becomes

$$\left(\frac{\ell}{1-n}\right)^2 \frac{\nu}{\gamma^3} \left(\frac{1}{2} + 2\ell n \frac{b}{a}\right) \ll 1 \tag{38}$$

or for typical parameters

$$\ell^{2/3} \ll \gamma$$

We see that Eq. (34) is quite generally accurate for $B_\theta^\circ = 0$.

V. THE ONR RACETRACK INDUCTION ACCELERATOR

The Office of Naval Research together with the Naval Research Laboratory have developed the design for a racetrack induction accelerator intended to accelerate a 1 kA (ν = 0.0588) electron beam to 40 MeV (γ = 80) in fifty revolutions. In an earlier report,[6] we investigated the beam breakup and negative mass instabilities for this design, concluding that the beam breakup instability poses few problems for induction module Q's of order six, a realistic value. The negative mass instability was found to be somewhat more threatening, although there was reason to hope that thermal effects would reduce the predicted growth rates, especially for large toroidal mode numebrs.[7] Our work was based on the dispersion relation of Ref. 2. Here, we repeat the analysis using Eqs. (23) - (27).

We treat the racetrack cavity as a torus of major radius R = 70 cm. (Straight sections of the racetrack are expected to have a favorable, but very small, effect on total negative mass instability growth.) Varying the assumed radius has little affect, because changes in the growth rate are approximately balanced by changes in the path length. In accordance with the accelerator design, the cavity and beam minor radii are taken to be b = 7 cm and a = 1 cm. A $B_\theta{}^\circ$ = 2 kG (ω_c = 1.73) guide field is applied.

The numerically determined growth rate for these parameters and ℓ = 13, a toroidal mode number near the upper end of the range for which the model is valid, is plotted as the solid curve in Fig. 2. The result from Ref. 6 is shown as a dashed line. The average growth rate is reduced by about a factor of two. Our more optimistic findings suggest a total negative mass instability amplification factor of fifteen e-foldings. This growth level probably can be reduced to an acceptable level (say, five e-foldings) by thermal effects or design changes.

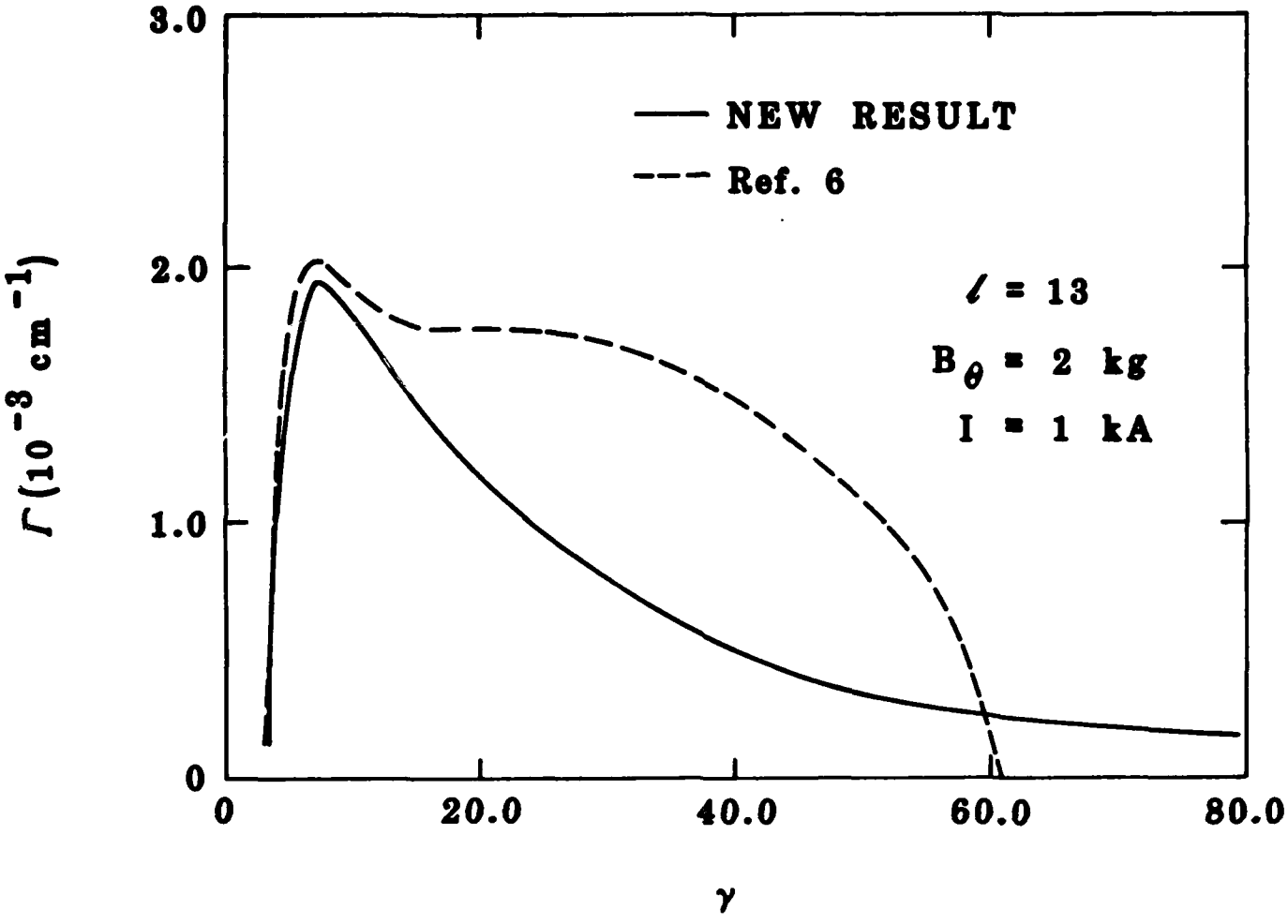

Figure 2. Predicted negative mass instability growth rate as a function of energy for the ONR racetrack induction accelerator design with a 2 kG guide field.

Figure 3 illustrates the corresponding $B_\theta° = 0$ growth rates. Peak values are reduced somewhat relative to the earlier results, but the high energy cutoff is shifted up in energy by a factor of twenty. For $\gamma \gtrsim 20$, Eq. (34) reproduces the solid curve well.

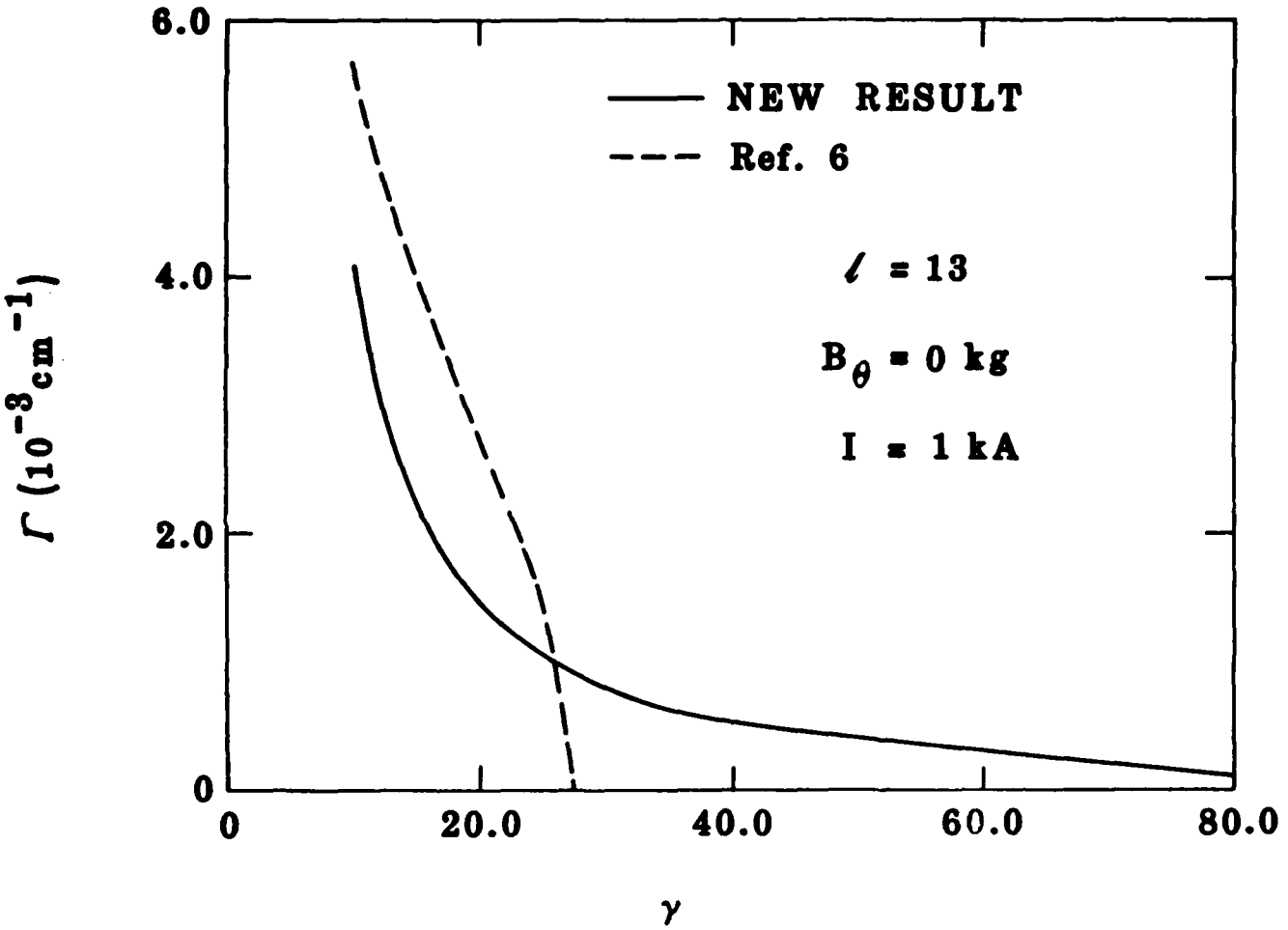

Figure 3. Predicted negative mass instability growth rate as a function of energy for the ONR racetrack induction accelerator design with no guide field.

REFERENCES

1. P. Sprangle and J. L. Vomvoridis, "Longitudinal and Transverse Instabilities in a High Current Modified Betatron Electron Accelerator," NRL-4688 (Naval Research Laboratory, Washington, 1981).

2. T. P. Hughes and B. B. Godfrey, "Linear Stability of the Modified Betatron," AMRC-R-354 (Mission Research Corporation, Albuquerque, 1982).

3. T. P. Hughes, M. M. Campbell, and B. B. Godfrey, "Analytical and Numerical Studies of the Modified Betatron," IEEE Nuc. Sci. NS-30, 2528 (1983).

4. T. P. Hughes, M. M. Campbell, and B. B. Godfrey, "Linear and Nonlinear Development of the Negative Mass Instability in a Modified Betatron Accelerator," Beams 83, to be published.

5. C. W. Roberson, "The Racetrack Induction Accelerator," IEEE Nuc. Sci. NS-28, 3433 (1981).

6. B. B. Godfrey and T. P. Hughes, "Beam Breakup Instabilities in High Current Electron Beam Racetrack Induction Accelerators," IEEE Nuc. Sci. NS-30, 2531 (1983).

7. P. Sprangle and D. Chernin, "Beam Current Limitations Due to Instabilities in Modified and Conventional Betatrons," NRL-5176 (Naval Research Laboratory, Washington, 1983).

8. T. P. Hughes, M. M. Campbell, and B. B. Godfrey, "Simulations and Theory of the Negative Mass Instability in a Modified Betatron," AMRC-N-247 (Mission Research Corporation, Albuquerque, 1983).

9. D. Chernin and P. Sprangle, "Transverse Beam Dynamics in the Modified Betatron," Part. Accel. 12, 85 (1982).

10. V. K. Neil and A. M. Sessler, Rev. Sci. Instr. 36, 429 (1965).

11. R. W. Landau and V. K. Neil, "Negative Mass Instability," Phys. Fluids 9, 2412 (1966).

12. B. B. Godfrey and T. P. Hughes, "Beam Breakup Instabilities in High Current Electron Beam Racetrack Induction Accelerators," AMRC-R-469 (Mission Research Corporation, Albuquerque, 1983).

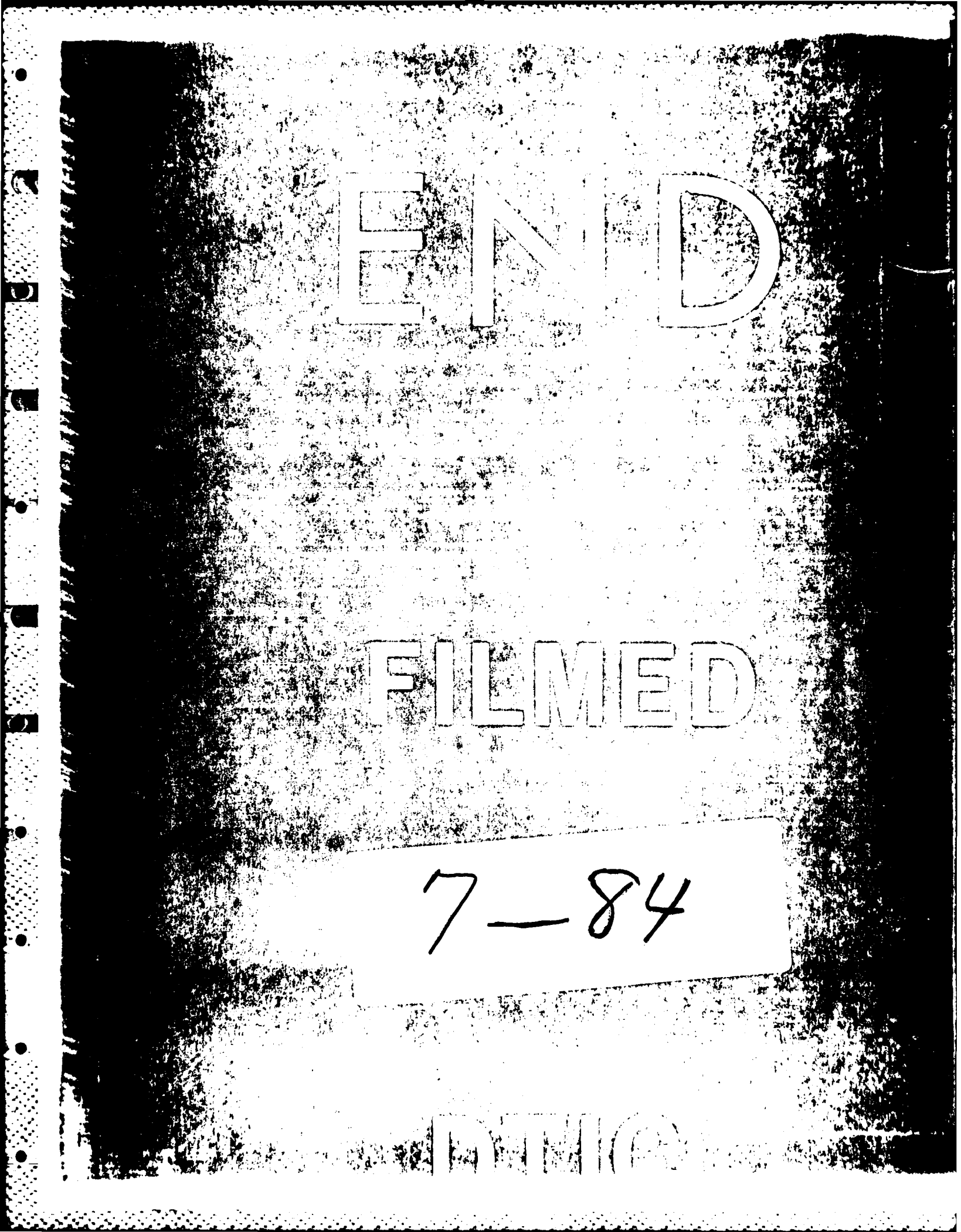
END
FILMED
7-84
DTIC